Est. 1984

ORIENTAL JOURNAL OF CHEMISTRY
An International Open Access, Peer Reviewed Research Journal

www.orientjchem.org

ISSN: 0970-020 X
CODEN: OJCHEG
2022, Vol. 38, No.(2):
Pg. 388-398

A Study on the Effect of Lawsone as Complexing Agent in the Electroless Zn-P Deposition

H. ASIA THABASSOOM[1]*, F. FEMINA, J. FELICITA FLORENCE[2], R. KANMANI and J. AMALA INFANT JOICE

*[1,2]PG and Research Department of Chemistry, Holy Cross College (Autonomous), affiliated to Bharathidasan University, Tiruchirappalli-620002, India.
*Corresponding author E-mail: asia.shahbir@gmail.com

http://dx.doi.org/10.13005/ojc/380221

(Received: January 31, 2022; Accepted: April 6, 2022)

ABSTRACT

The effect of *Lawsonia inermis Linn* Leaf extract on electroless deposition of Zinc-P alloy on mild steel is studied in alkaline solutions. The effect of experimental processing parameters on the deposition rate is investigated during electroless plating. The bath compositions and operating conditions are optimized. The results obtained show the inclusion rate of electroless Zn-P alloy coating is found to be increased by increasing the volume of additives from 0.5 mL to 1.5 mL. Structured UV-A significant spectroscopic absorption rate is taken to ensure the presence of Lawsone in the binary complex in the alkaline bath. In the absence of a complexing agent, additive Lawsone develops more features and levels of arrangement. It offers the idea of changing sodium citrate with Lawsone. The effect of Lawsone as a complex agent on Zn-P electroless coating is tested by SEM, EDAX, AFM, XRD and corrosion studies. The corrosion efficiency of electroless Zn-P coating is assessed by polarization and electrochemical impedance spectroscopy.

Keywords: *Lawsonia inermis Linn* leaf, SEM, EDAX, XRD, AFM, Micro hardness, UV-Visible spectrum and polarization studies.

INTRODUCTION

Electroless plating of metals and process technology have important role along with other methods of plating. Electroless process is not constrained by the shape, size or conductivity of the supporting substance[1-3]. It is a highly effective means of plating metals into nonconductors. Hence electroless plating has elicited much interest among scientific community in recent years. Today, sophisticated electroless plating systems are in use in many varied electronic applications (PCB industries, IC fabrication, EMI shielding etc)[4].

Electroless plated zinc coatings are considered as one of the many ways of corrosion protection of steel. Zinc has many functions. It is widely used in a variety of covering methods for the protection of various metals, as well as in powder and dust formulations, such as oxide, and for clinical purposes[5]. Zinc is cut into dry batteries and hardens the copper covering the U.S. penny. Zinc alloys are

often combined with various metals that allow you to be strong and durable[6-8]. Zinc shields prevent the oxidation of the coated metal by forming a barrier and acting as a sacrificial anode when this limit is damaged. Electroless plating installation applies to materials requiring solid, high-resistant corrosion. This makes the process ideal for the oil or marine industries. Parts such as pumps or valves for decaying agents will usually be better suited to be fitted with electroless plated[9-10].

It is apparent from the literature that the single addition agent generally does not produce good deposit. In order to get good deposit, two or more addition agents are required[11-13]. The presence of more addition agents poses problems in determining their consumption during plating. Additionally some of the addition agent cause pollution problem and health hazard. The use of local plant, *Lawsonia inermis Linn* (henna) leaf extract, as addition agent in zinc-Phosphorous electroless deposition from alkaline bath, in this work, makes this study significant[14-16]. Henna coloring properties are due to Lawsone, a burgundy organic compound that has an affinity for proteins. Lawsone usually focuses on the leaves, especially among the leaf petioles[17]. The polarization method is used to produce liquid extracts of henna leaves as a corrosion inhibitor of carbon steel, nickel, and zinc in acidic, neutral, and alkaline solutions reported elsewhere[18-20]. This hair care plant is reported to have immunomodulator, anti-inflammatory, antimitotic, analgesic and anti-inflammatory, and carcinogenic and antioxidant properties. Henna is an important photochemical source of great medical and medicinal value. Lawson's molecular formula is $C_{10}H_6O_3$ and its melting point is 190°C. It exists in three tautomeric forms; 1,4-naphthoquinone structure is the most stable form followed by 1,2-naphthoquinone and 1,2,4-naphthotrione; the trione system is slightly stable. In the present paper, Lawsone dye separated from the henna extract is used as an electroless complexing agent in the Zn-P bath shower. It is also very eco friendly and its successful use as an additive and as well as complexing agent, in the improved electroless deposition of zinc-Phosphorous on mild steel, will be technologically and economically beneficial. This paper explains the preparation and characterization of electroless Zn-P alloy thin films.

EXPERIMENTAL

Materials

A specimen of mild steel in the form of (10cm x 6cmx1mm) is used. The chemical composition is as the follows: (wt %)

C (0.15%); Si (0.25-0.75 %);
P (0.07-0.15%); Al (0.015-0.06%);
Cu (0.25-0.55 %); Ni 0.65%

Surface preparation

The Specimen is mechanically cleaned to ensure removal of unwanted dust, followed by degreasing in acetone. The substrate is thereafter cleaned in 10% NaOH solution at 10 min then the substrate is dipped in 10 mL of con. HCl for 2 min resulting in etching[21].

Bath composition

The binary Zn-P alloy coating is prepared with a composition of 90wt.% Zn and 10wt.% P using the electroless plating bath. Zinc sulphate acts as a source of metal, sodium hypophosphite is taken as a reducing agent and sodium citrate is used as a complexing agent. The ammonium chloride in the bath composition itself acts as a buffer[22].

Table (A): Bath formulation in the electroless Zn-P alloy

Bath Composition	Concentration
Zinc Sulphate Hepta hydrate	0.40-0.70 g/L
Sodium hypophosphite	0. 30 g/L
Sodium citrate	0.25 g/L
Ammonium Chloride	0. 50 g/L
Operating Conditions	Temperature (70-90)^{0}C pH-(7-8) Plating time-2 & 1/2 h

Preparation of bath solution

The above chemicals are taken in a 400 mL beaker. The chemical mixture is dissolved in double distilled water. The clear solution is taken into the 500 mL standard flask and make up into the mark line. The electroless plating is done by two and half hour duration on mild steel specimens. Then Electroless plating in noted. The rate of deposition is also calculated by using the formula,

$$\text{Rate of deposition} = \frac{\text{Weight of the deposit X } 10^4 \text{ X } 60}{\text{Area X Density X Time}} \quad (1)$$

Coating characterizations

The surface nature of Zn-P films was characterized by SEM and AFM. The elemental content of deposits of films was examined by Energy dispersive X-ray spectroscopy and crystal structure of deposits was analyzed by X-ray diffraction study. The micro hardness of films was measured by Vickers Hardness Test. The corrosion behavior is evaluated by potentiodynamic polarization curves.

Isolation of Lawsone

Tommasi's procedure: Powder of dried henna leaves (500 g) is placed in a 5 litre Erlenmeyer flask containing a magnetic bar and distilled water (2500 mL) is added. The suspension is stirred on a magnetic stirrer with heating while the temperature is kept around 80°C. After around 2–3 h, the colour of the green suspension turned brown. The suspension is left overnight. After that lime water is added until the suspension turned alkaline. The suspension is filtered by gravity over several large glass funnels with filter paper. The filtrates are combined and acidified to pH 3 by addition of 0.12 M HCl. The filtrate is extracted with diethyl ether (3 × 1000 mL). The combined ethereal phases are washed with water (3 × 1000 mL) and dried over anhydrous $MgSO_4$. After the removal of ether on a rotary evaporator, more or less a reddish solid material is obtained as crude product (3.25 g). The progress of the isolation of Lawsone is monitored by IR spectroscopy and TLC on silica gel. Column chromatography on silica gel 60 with a mixture of EtOH: EtOAc (1:2 v/v) as the mobile phase resulted in the formation of different colour zones. The crude product (0.5 g) was dissolved in 10 mL of the eluent and placed at the top of the column and the elution was started. Fractions of 10 mL were taken. Almost 50 fractions were collected. The compositions of all fractions were monitored by Thin layer chromatography.

RESULTS AND DISCUSSION

The Electroless plating has been described as a reduction process based on the autocatalytic reduction process of metal ions in an aqueous solution containing a chemical reduction agent. Electroless Zn-P alloy plating research is gaining great importance due to its corrosion resistance. The current study aims to produce an electroless Zinc-Phosphorous alloy coated with a mild metal using Sodium hypophosphite as a reducing agent. Ammonium chloride as a buffering agent and Lawsone separated from *Lawsonia inermis Linn* leaf acts as a complex agent.

Table (B): basic bath for electroless Zn-P plating

Zinc sulphate hepta hydrate	0.40-0.70 (g/L)
Sodium hypophosphite	0.30 (g/L)
Ammonium chloride	0.25 (g/L)
Sodium citrate	0.50 (g/L)
Temperature	70°C-90°C
PH	7-8

Effect of addition agent (Lawsone)

Lawsone leaves contain a natural and highly effective coloring agent. Lawsone dye molecules color hair and skin by attaching them safely to their protein molecules[23]. The effect of the additive agent is investigated by adding 0.5-2.5 mL of Lawsone to the base bath of electroless Zn-P alloy deposition. Lawsone additions at 1.5 mL have a high concentration. This ensures the addition of Lawsone which changed the level of Electroless deposition and produced a bright Zinc-P deposit of soft metal alloy. Additive concentration intensified to 1.5 mL.

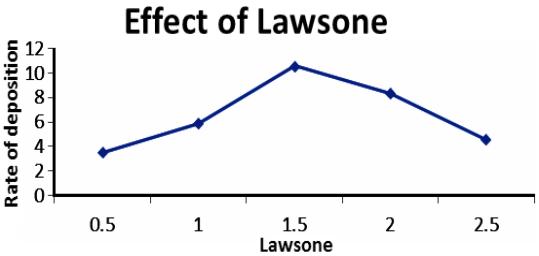

Fig. 1. Effect of Lawsone

Effect of zinc sulphate on rate of deposition

Zinc Electroless Plating provides corrosion resistance by acting as a barrier and covering the victim. There was a close relation between the concentration of Zinc sulphate and appearance of plating layer in cell experiment. Veeraraghavan *et al.,*[24] reported that in order to get high corrosion resistance a bright Zinc deposit, to find out the effect of Zinc ion, the Zinc sulphate concentration is varied from 1-10 g L^{-1} keeping Henna Extract at 1.5 mL. At lower concentrations dull deposits is observed in the rate of deposition. As well as concentration is high bright deposits is observed in the rate of deposition. Fig. 2B shows that with increase in the concentrations the brightness range is extended to higher and lower rate of deposition.

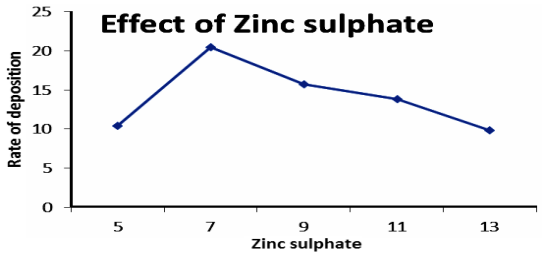

Fig. 2. Effect of Zinc sulphate

Effect of sodium hypophosphite monohydrate

Sodium hypophosphite is the sodium salt of hypo phosphorous acid. It is found from the table when the concentration of sodium hypophosphite monohydrate is increased, the rate of deposition is also increased. Increasing the H_2PO_2- concentration increases the phosphorous content of the deposit. In Fig. 3 When the concentration of $NaH_2PO_2.H_2O$ is 4g/L the rate of deposition is 3.31μ/h higher compared to various concentrations of Sodium hypophosphite monohydrate. Thus, 4g/L is taken as the optimum concentration.

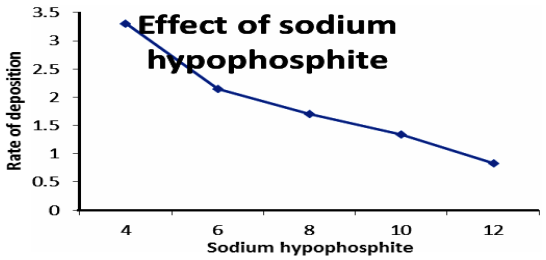

Fig. 3. Effect of sodium hypophosphite

Table 1: Effect of Lawsone

S.No	Lawsone	Rate of deposition
1	0.5	3.5
2	1	5.86
3	1.5	10.54
4	2	8.3
5	2.5	4.6

Effect of sodium citrate

Sodium citrate is the sodium salt of citric acid. It is white, crystalline powder or white, granular crystals, slightly deliquescent in moist air, freely soluble in water, almost insoluble in alcohol. Sodium citrate is used as a complexing agent during zinc deposition[25]. Fig. 4 shows that the highest zinc deposition rate is obtained at 3g/L sodium citrate. The increasing the concentration of sodium citrate 3g/L increases the deposition rate. At low sodium citrate concentration the bath is unstable and spontaneously decomposes; this is because citrate is a strong complexing agent used to prevent the precipitation of zinc hydroxide or basic zinc salts which have a negative effect on the deposition rate. The results show that the citrate concentration has an adverse effect on the deposition rate (DR) and the surface roughness (Ra).

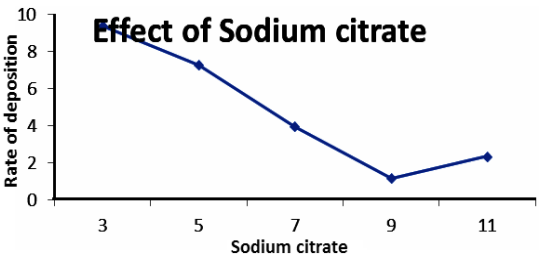

Fig. 4. Effect of sodium citrate

Table 2: Effect of Zinc sulphate

S.No	Zinc sulphate	Rate of deposition
1	5	10.45
2	7	20.53
3	9	15.78
4	11	13.83
5	13	9.85

Effect of ammonium chloride

Ammonium chloride helps with pH and has a mild effect on abortion. It is an inorganic chloride and ammonium salt. When the concentration of Ammonium chloride is increased the spraying rate increases and is found to be 2g/L. Therefore, a bath containing 2g/L of Ammonium chloride is considered a high concentration of electroless zinc alloy deposition.

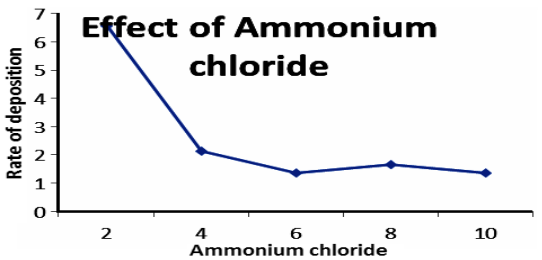

Fig. 5. Effect of Ammonium chloride

Table 3: Effect of sodium hypophosphite

S.No	Sodium Hypophosphite	Rate of deposition
1	4	3.31
2	6	2.15
3	8	1.7
4	10	1.34
5	12	0.83

Effect of temperature and ph

Typically, the Zinc-free storage area rises sharply when the temperature rises from 50 to 80°C raises the temperature from 50 to 80°C and increases the storage rate. At high temperatures, however, the cover seems to fade. The effect of temperature on the electroless bath is very essential as it produces the energy needed for the chemical bonding occurring from the metal oxidation. So the ideal temperature for inactive Zinc is 70°C. Placement level increases significantly with an increase in pH from 4 to 8. It is found in Fig. 5 where Temperature and pH are raised the storage level rises and reaches 700c and pH 7.

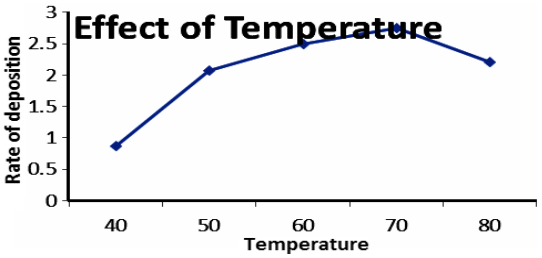

Fig. 6. Effect of temperature

Table 4: Effect of sodium citrate

S.No	Sodium Citrate	Rate of deposition
1	3	9.38
2	5	7.27
3	7	3.95
4	9	1.16
5	11	2.34

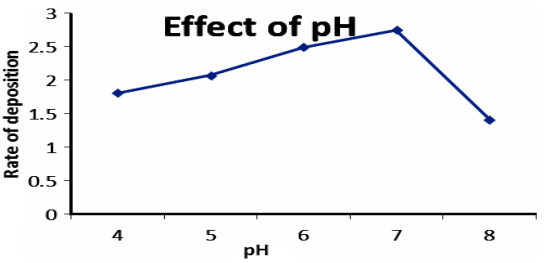

Fig. 7. Effect of pH

Table 5: Effect of Ammonium chloride

S.No	Ammonium chloride	Rate of deposition
1	2	6.58
2	4	2.14
3	6	1.36
4	8	1.67
5	10	1.35

Effect of plating time

It is located on the graph when the plating time is increased and the placement level rises and is found to be 150 min long. This is considered to be the ideal time to consolidate electroless zinc alloy deposition. In addition, extending the inclusion period is not economically attractive for industrial applications.

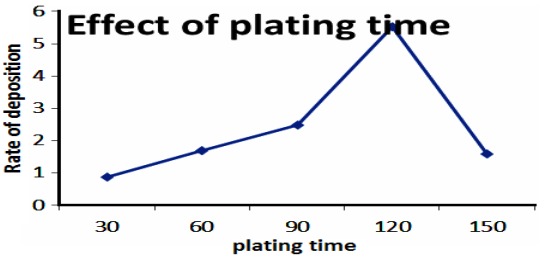

Fig. 8. Effect of Plating Time

Table 6: Effect of Temperature

S.No	Temperature	Rate of deposition
1	40	0.87
2	50	2.07
3	60	2.49
4	70	2.75
5	80	2.21

Optimized bath composition

By varying the various bath components in the presence of additive, based on the rate of deposition the bath composition is optimized for electroless zinc alloy deposition in the presence of an additive Lawsone.

Effect of Lawsone in the absence of complexing agent

The effect of Lawsone, an additive on electroless Zn-P alloy, is measured, in terms of setting where there is no complex sodium citrate agent. It is found that the suspension level increases and the magnitude also increase when Lawsone is added from 0.5 mL to 1.5 mL when there is no sodium citrate (0g/L). So Lawsone acts as a complex agent. As the deposition rate increases, more magnitude increases.

Adsorption process by UV–Visible spectra data

The UV-Visible spectrum measurement is performed to study the state of complex matter in the solution. Absorption at a wavelength from 250 to 850nm is measured at room temperature. To identify the complex ion in the electroless Zn-P deposition Fig. 1 shows the iron of Zinc sulphate aqueous solution and the sodium hypophosphite reducing agent with their first peak at 283nm, with band

intensity; and also the addition of a complex sodium citrate agent top position moved to 286nm. This meant that there is a complex formation of Zn-citrate ion in Fig. 1. Gradually add Accelerator ammonium chloride and peak position moved to 285nm with band intensity indicating Zn-ammonia complex spectrum ion. At pH of 7, the spectrum of Zn-citrate (286nm) and Zn-ammonia (285nm) complexes, therefore, this peak can be considered Zn-citrate-ammonia complex. The spectrum of ion complex in the plating solution is given to fig. Zn peaks switched to 283 and 285nm to obtain alkaline solutions (pH 7). Therefore, Lawsone, the supplement is added to the top position moved to 294nm in the empty Zn-P zone showing Zinc-Lawsone complex ion formation in fig. Lawsone acts as a complex agent. Zn-Lawsone, however, has switched to higher wavelengths than those seen in other complex ions. The additional installation of Electroless Zn-P and Lawsone, the addition increases light absorption. The maximum frequency ranges from 283 to 294nm, band intensity increases and reaches a maximum of 294nm.

Morphology of electroless Zn-P deposits

Surface morphology, crystal growth and Zn-P non-electrical deposit structure are tested under high magnification using an electron scanning microscope. The scanning electron microscope, which uses the reflected electron and the second electron, allows a person to obtain information from areas that cannot be explored by others[25]. SEM images of Zn-P non-electric as deposit for 150 min, given in Fig. 9 respectively in dual magnification x100 & x300. We have less crystals with increased size and large number. Nodular grains fully covered the surface of pores. The Zn-P and Lawsone Deposit made up of 150 minutes of the deposited plate have the same smooth surface texture. Planned samples are also recognized for physical appearance.

Fig. 9. Represents bath contains without sodium citrate

EDAX analysis

The electroless zinc is deposited by an autocatalytic chemical reaction between the Lawsone and citrate solution. The overall chemical reaction can be represented as follows

$$2[H_2PO_3]- + Zn^{2+} + + H_2O \rightarrow [HPO_3]_2 - + Zn+P + 1/2H_2 \uparrow + 2H2O \quad (2)$$

The formation of a non-electronic deposit is measured using EDAX. Fig. 10 shows the effect of refining time on% P and Zn on coatings[26]. When the setting time increases from 30 min to 150 min, in % P it decreases to a certain level, which may be due to a decrease in H+ions. In addition, % of Zn has increased.

$$2H_{ad} \rightarrow H_2 \quad (3)$$

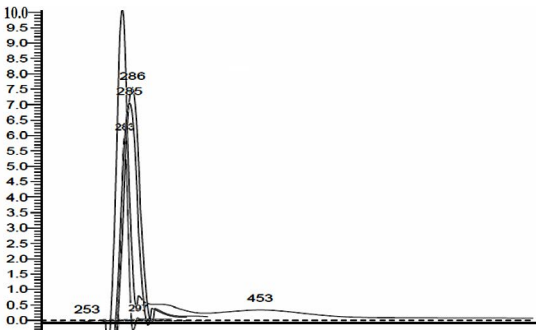

Fig. 10. In the UV spectrum variation of BB, OB, with and without of sodium citrate

Table 7: Effect of plating time

S.No	Plating time	Rate of deposition
1	30	0.87
2	60	1.68
3	90	2.49
4	120	5.53
5	150	1.59

EDAX spectra of electroless Zn-P coatings made for 150 min are shown in Fig. 11. The EDAX spectrum at 150 min of setting time shows Zn and P peaks. Elevated zinc comes from alkaline baths. The EDAX spectra show the height of Zn and P only. As the wear time increases, the zinc level rises. From the spectra, the presence of Zn and P is seen in the coating as a deposit. This, however, creates the advantage of using Zinc to build worn parts in machinery.

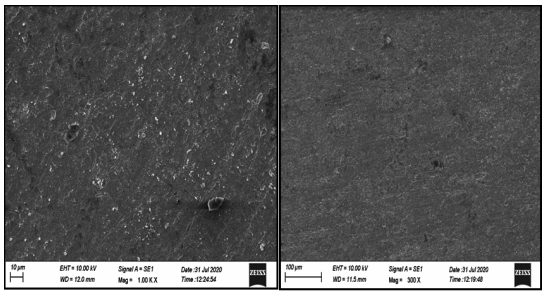

Fig. 11. EDAX spectra for basic bath and optimized bath

Table (C): Optimized Bath Formulation for Electroless Zn-P plating

Zinc Sulphate hepta hydrate	7 g/L
Sodium hypophosphite	4 g/L
Ammonium chloride	2 g/L
Lawsone (2-Hydroxy-1,4-Napthoquinone)	1.5mL
Sodium citrate	3 g/L
pH	7
Temperature	70°c

Surface analysis by AFM

Figure 12 shows AFM (a) top view (2D) (b) three-dimensional (3D) views and (c) a detailed profile of Zn-P's non-electric clothing embedded in Lawsone in minutes -150 respectively. According to an AFM image, the surface morphology of electroless Zinc coating appears at short intervals. Constructed deposits with the rapid growth of nodules and structural structure in fig., fast-growing behavior is nothing but more robust. b) Analyzing the deep profile in a horizontal surface Fig. shows small peaks in the surface of the measured surface for 50m. The maximum distance is measured by the 'X-axis and gives the size of a particular crystal. The crystal size is less than 50nm[27]. The AFM images in Fig. (4b) reveal that the adhesion formed during the 150-min suspension, the growing Electroless Zn-P crystals are very smooth and well marked with the same deposit and morphology. An in-depth profile analysis in the horizontal area Fig. shows small peaks in an approximate area of 50µm. No sharp peaks are available, i.e. coating is naturally amorphous. The grain size is less than 50nm. The rate of local decomposition (Ra) of the Zn-P installed in Lawsone according to AFM standards is 108.3nm for 150 min of the prepared bath time and 219.0nm for the basic installation time of 150 min respectively.

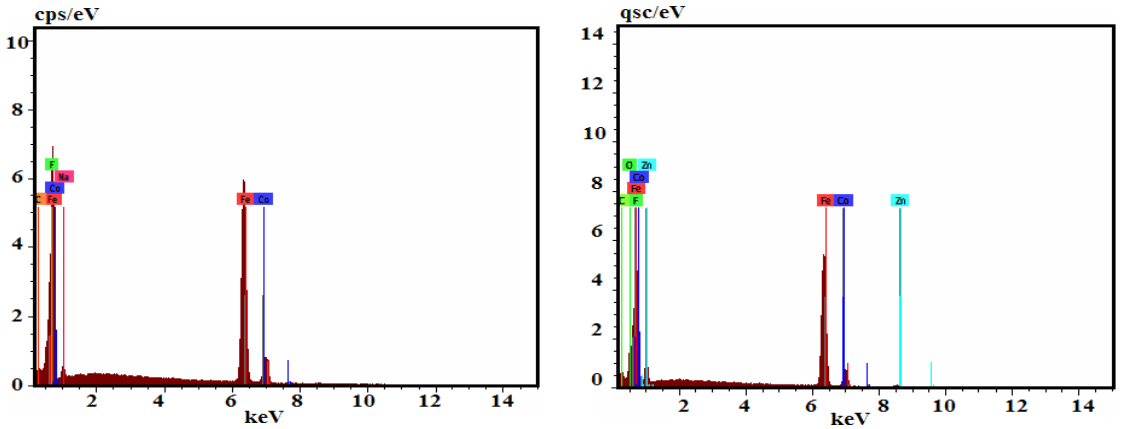

Fig. 12. EDAX spectra for basic bath and optimized bath

Table (D): Optimization Bath for without sodium citrate

Zinc sulphate hepta hydrate	7 g/L
Sodium hypophosphite	4 g/L
Ammonium chloride	2 g/L
Lawsone(2-hydroxy1,4 Naphthoquinone)	1.5 mL
pH	7
Temperature	70°c
Plating time	21/2

X-ray diffraction studies

Figure 13 shows the X-ray patterns of Zn-P non-electric diffraction obtained from a prepared non-electric bath and basic bath for 150 consecutive minutes. It appears in Figs.11 & 12 that sharp peaks appear to be approximately 38°, 45°, 64°, 83°, corresponding to P (310), Zn (111), P (200), and Zn (222) after 150 min of installation time. Height shows a distinct cubic expression (hkl) corresponding to the cubic centered surface and other structures. These results suggest that the crystal planes seen in these drawings are enlarged in accordance with the texture of the substrate. From Fig. 14 for bath time, different textures are developed, such as P (310) from 38°, Zn(111) at 45°, P(222) at 64° and Zn(220). The XRD pattern reveals a wide range of 2θ values of 40-50°, indicating that Zinc-phosphorous alloys are naturally amorphous. It has been widely found

that new bath deposits have fine glossing properties but deviate from crystalline expansion and growth and thickening[28]. Sharp heights are found in (111) diffraction of nanocrystalline Zn and wider heights are found in the separation of the amorphous phase or the nanocrystalline phase in the non-electrical Zn-P deposit. In the case of a prepared bath using the 1.6° FWHM and Scherer equation, the grain size is estimated at 81.80nm. Size is calculated using the Scherer equation.

$$D=B\lambda/\beta \cos \Theta \quad (4)$$

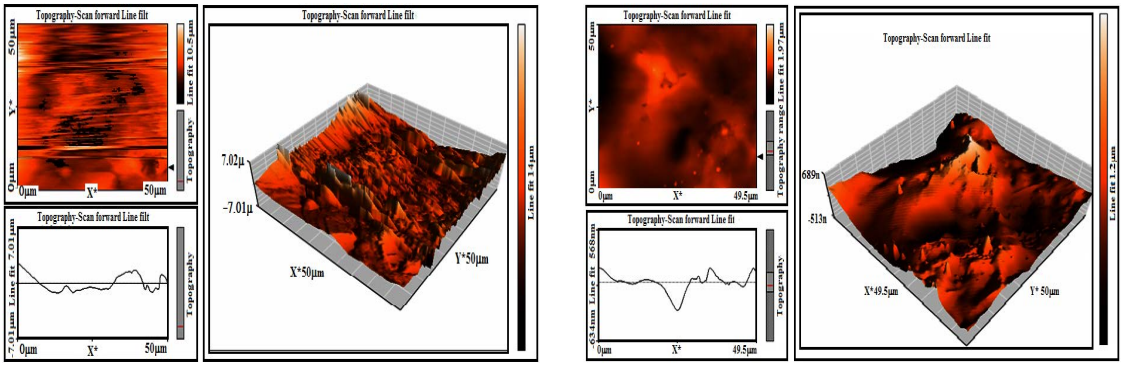

Fig. 13. AFM images of as-deposited electroless Zn-P coating on Lawsone (a) Topographic image (b) 3-Dimensional and (c) Depth profile analysis image

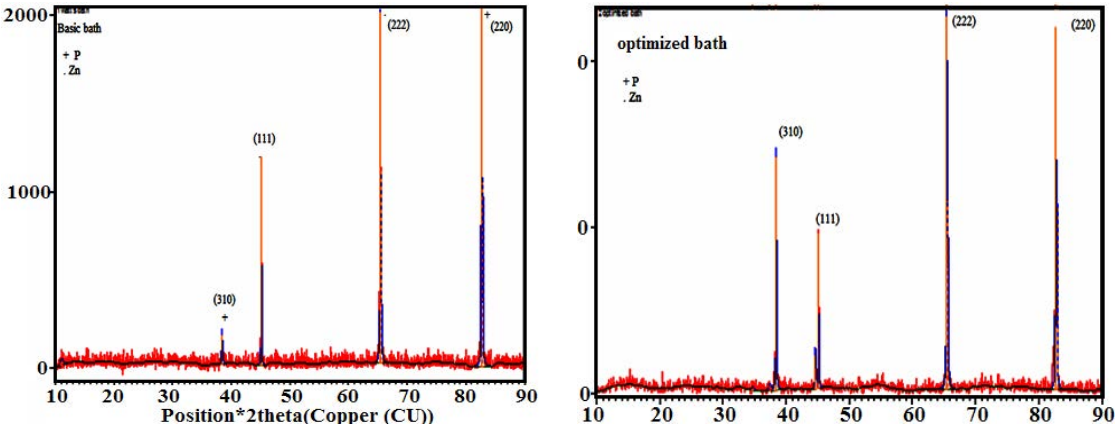

Fig. 14. XRD patterns for basic bath and optimized bath

Table 8: Absorbance studies

S.No	Bath	Absorbance
1	Basic bath	283nm
2	Optimized bath	294nm
3	Ni-cit complex bath	286nm
4	Ni-ammonia complex bath	285nm

Where D is the average crystallite size of phase under investigation, B is the Scherer constant (0.89), λ is the wavelength of X-ray beam used, β is the full-width half maximum(FWHM) of diffraction and θ is the Bragg's angle.

Micro hardness

Strengthening material that provides resistance to retreat or scratching. Stiffness is usually characterized by strong intermolecular bonds[29]. The durability values provide a comparable level of resistance to flexibility of the plastic from a standard source, as special durability techniques have different dimensions. Vickers' strength test is a commonly used test because of its wide range of load capacity. Vickers (HV) Strength is calculated as:

$$HV = 1.8544F/d^2 \quad (5)$$

Table 9: Edax analysis

Type of deposited coating	Zinc (Wt %)	Phosphorous(Wt %)	Carbon (Wt %)	Oxygen(Wt %)	Iron(Wt %)
Zn-P basic bath	61.46	8.99	7.45	7.27	39.03
Zn-P optimized bath	63.62	9.47	8.11	10.53	51.53

When the load (F) is strong in Kilogram and the definition of two diagonals created by the pyramid indent (d) is a millimetre. The slightest difficulty in testing the Zn-P coatings is made with a small UHL hardness test (VMHT MOT, Sl. No. 1002001, and Technische Microscopy) with a Vickers diamond backing. Ni-P is a small durability test by using an accurate diamond indenter with a load of 1kgf. The sitting time is set at 10 seconds while the reversal speed is set at 50μm/s. It should be mentioned here that the stiffness is measured as soon as the wear is finished with Lawsone with or without it and no separate adjustments are made. An estimate of at least three values of the solitude of each sample is reported in graph 1. It may also be referred to that the depth of retrospective (h) is related to the diagonal definition (d) in relation.

$$h=d/7 \quad (6)$$

In the present test, the maximum d value is found to be approximately 46μm. Therefore, h is measured as 46/7=6.57μm. Therefore the depth of the indent is very small compared to the thickness of the cover. This means that the relative strength of the rubber represents the hardness of the rubber itself without the impact of the substrate material to come.

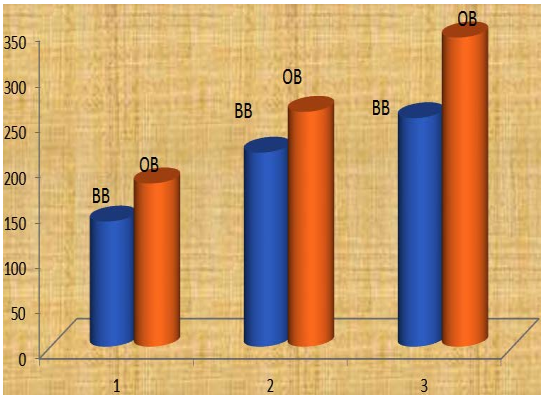

Fig. 15. Micro hardness of electroless Zn-P deposition

Table 10: polarization study

Bath	E_{corr}	I_{corr}	b_a	b_c
Basic bath	-812.597mV	27.976μA	52.458 mV	78.199 mV
Optimized bath	-900.188mV	13.402μA	215.875 mV	57.761 mV

Corrosion resistance of electroless deposited Zn-P alloy coating

To check the corrosion resistance of the Zn-P alloy coating installed (internal and external) an extension is used. A Zn-P mixture of the same thickness was added to the 10% NaOH and 3.5% NaCl solution for 12 days. The degree of corrosion of this alloy is calculated by weight. Details are shown in the table. It has been found that corrosion resistance with Zn-P alloy coating in front of Lawsone (OB) shows better than in the absence of Lawsone (BB) Corrosion resistance. The rust strength (E_{corr}) is 812.597mV and the rust density (I_{corr}) is 27.976 μA. The rust strength has changed dramatically at 900.188mV in the Zn-P where there is a soft expanded metal in the optimized bath[30]. E_{corr} value of OB is higher than BB value. So, OB is having better corrosion resistance. This particular study justified the good Corrosion resistance of the layer which was formed on the mild steel surface in the presence of Henna extract.

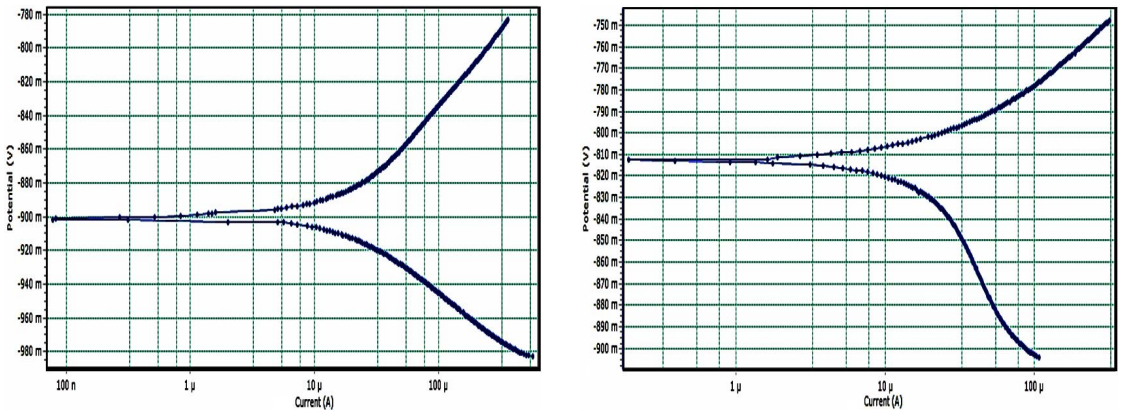

Fig. 16. polarization studies

Table 11: Ac impedance study

Bath	Centre point X	Centre point Y	Diameter	Sample deviation	Depression
Basic Bath	2.6871	2.2738	5.6003	0.0767	-54.296°
Optimized bath	2.5512	2.1465	6.5495	0.0667	-40.995°

Zn-P adhesive polarization curves with the same thickness in 10% H_2SO_4 solution are shown in Fig. The Electrochemical corrosion parameters found in it are listed in the table. It is clear from Fig. 16 that as the Zn-P alloy deposit has very high corrosion strength, E_{corr} and corrosion current density is very low I_{corr}. Therefore resist further corrosion in prepared bath deposits. The compressed single semicircle is similar in shape but varies in width. The diameter of the semicircle determines the rust resistance and the surface thickness. This has shown the effect of additive Lawsone on deposits.

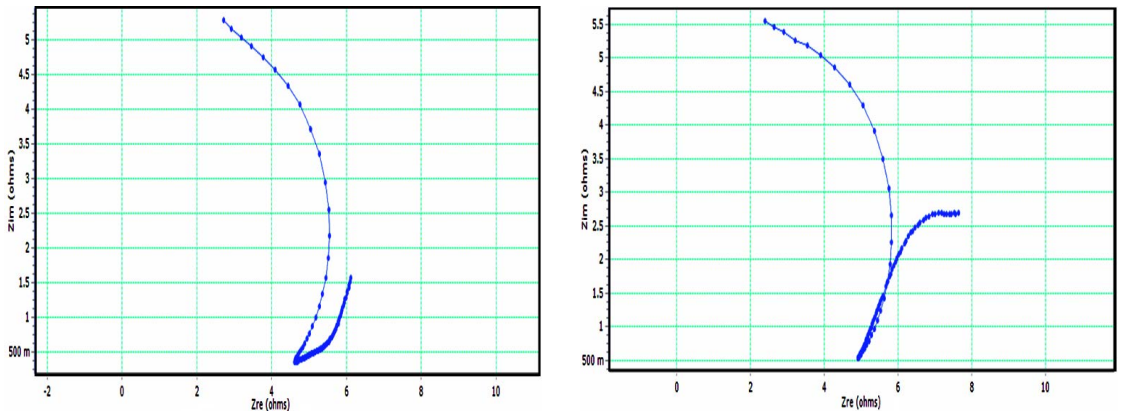

Fig. 17. Impedance studies

CONCLUSION

The Zinc-Phosphorous alloy deposits on mild steel obtained from this optimized bath has shown better characteristic properties than the Zinc-Phosphorous alloy deposits obtained from Basic Bath. This confirms the influence of *Lawsonia inermis* extract on electroless deposition of Zinc-phosphorous alloy. The fine grained deposits on Zinc-phosphorous alloy electroless plated mild steel from optimized bath reveal the inclusion of addition agent on Zinc-phosphorous alloy electroless deposition. XRD spectra reveals the reduction in the particle size of Zinc-phosphorous deposits on mild steel obtained from optimized bath. EDAX analysis confirms the inclusion of *Lawsonia inermis* Extract on Zinc-phosphorous alloy electroless plated mild steel from optimized bath and it reveals that Zinc percentage in this deposition is 63.65%. Hardness value is also increased for zinc electroless plated mild steel from optimized bath. Potentiodynamic polarization studies were performed and showed that all coatings had good resistance to 3.5% sodium chloride solution. The potentiodynamic polarization study of Zn-P without electricity changes E_{corr} and I_{corr} to the positive side ensuring higher Lawsone performance. Thus *Lawsonia inermis Linn* leaf extract acts as a Green addition agent and also it can satisfy the properties of the good addition agent. It is eco friendly, nonhazardous addition agent and it has many medicinal properties.

ACKNOWLEDGEMENT

I thank our institute Holy cross college of Trichy, Bharathidasan University for providing Laboratory and library facilities.

Conflicts of interest

The authors have no conflict of interest.

REFERENCES

1. Warner J.C.; Brandt D.A. Metallurgy Fundamentals. Good heart Wilcox Co., USA **2005**.
2. Spirano. S.; Verne's.E.; Faga MG.; Bugliosi.; Giovanni Maina. *Science Direct.*, **2005**, *259*(7-12), 919-925.

3. Tharamani.C.N.; Shafia Hoor.; Noor Shahina Begum.; Mayanna.S.M. *Journal of Solid State Electrochemistry.*, **2005**, *9*(7), 476-482.
4. Talbot D.E.J.; Talbot J.D.R. *Corrosion science and Technology*. 2nd. CRC Press., **2007**.
5. Winston R.R.; Herbert.H. *Corrosion and corrosion control, an introduction to corrosion science and Engineering (fourth edition). A John Wiley & Sons, Inc., Canada.*, **2008**.
6. Kanokwan Saengkiettiyut.; Pranee Rattanawalee dirojn.; Supin Sangsuk. *Special Issue on Nano Technology.*, **2008**, *7*(1), 33-36.
7. Abdel Hamid.Z.; Hassan.H.B. Attica.A.M. *Surface and Coating Technology.*, **2010**, *205* (7), 2348-2354.
8. P. Sahoo.; S.K Das, *Tribiological of electroless nickel coatings- A review, Mater. Des.*, **2011**, *32*(4), 1760-1968.
9. Ash agar. A.; Shiri. A. *International Journal of ChemTech Research.*, **2011**, *3*(4), 1941-1944.
10. Mahmoud.S.S. Ahmad Saatchi.; *Mustafa Alisha. Applied Surface Sciences.*, **2012**, *258*(7), 2439-2446.
11. Yongxin Li.; Prathish Kumar.; Xianming Shi.; Tuan Anh Nguyen.; Zhenjian Xiao.; Jianlin Wu. *Int. J. Electrochem. Sci.*, **2012**, *7*, 8151–8169.
12. Sappinandana Akamphona.; Sittha Sukkasib.; Yuttanant Boonyong maneerat. *Conservation and Recycling.*, **2012**, *58*, 1-7.
13. Laurence.W.Mckeen. *Introduction to Flouropolymer.*, **2013**, 231-276.
14. Santhosh Yadav Anilkumar.; Ashok Kumar. *International Journal of Pharmaceutical of Chemical Sciences.* **2013**, *2*(2).
15. Chulaluk Somphotch.; Suparoek. Henpraserttae. *Journals of metals.*, **2014**, *24*(2).
16. Osifuye1.C.O.; Popoola1.A.P.I.; Loto1.C.A.2.; Oloruntoba1D.T. *International Journal of Electrochem. Sci.,* **2014**, *9*, 6074–6087.
17. Karina chouchane.; Alexandra Lévesque.; Omar Aaboubi. *International Journal of Material Research.*, **2015**, *106*(1), 52-59.
18. Zhao, Yazoo G.L.; HaoY.L. *Metallurgy and materials.*, **2015**, *60.*
19. Mohd Imran Ansari.; Thakur Dr.D.G.; *International Journal for Technologies Research in Engineering.*, **2015**, *2*(7).
20. Zhao.G.L.; Zhou's.; Hao.Y.L.; Zou Z.D.; *Archives of metallurgy and materials.*, **2015**, *60*(2).
21. Loto.C.A.; *Springer science.*, **2016**, *8*, 177-186.
22. Azmah Hanim. M. A.; Noor Akmal.; Fadil Siti Rabiatull Aisha. *International Journal of Engineering& Technology.*, **2016**, *8*(6), 2558-2570.
23. Mohd Imran ansari.; Dinesh Singh G. Takur. *Engineering Science & Technology an International Journal (in press).,* **2016**.
24. Veeraraghavan B.; Haran B.; Prabhu S & Popov B, *Journal of Electrochemical Society.,* **2003**, *150*, 131.
25. Sahib Mohammed Mahdi., *International journal of Energy and Environment.*, **2017,** *8*, 321-330.
26. Seyyed Hashem Mousavi Anjidan.; Masoud Sabz.; Mustafa Rohani Zade.; Mansour Farza. *Materials Research.*, **2018**, *21*(2).
27. Roung Hu.; Yongyao Su.; Yurong Liu.; Hongdong Liu., *Nanoscale Research Letters.,* **2018**, *13*, 198.
28. Latha.N.; Raj.V.; Selvam.M.; Manisankar. P., *International Journal of Chemical Science* ., **2012**, *10*(1), 479-489.
29. Allah karam S.R.; Zarebidaki.A.; Rabizadeh.T.; *International journal of Modern physics.*, **2012**, *5*, 817-824.
30. Ram Kumar.; Manoj Kumar.; Sourabh Maheshwary.; Sulaxna Sharma.; Awnaish Sharma., *International journal of Advanced research i n Science and Engineering.*, **2018**, *7*.